



Research paper

Metabolomics study of ribavirin in the treatment of orthotopic lung cancer based on UPLC-Q-TOF/MS

Shihao Zhu¹, Xiang Han¹, Ruiying Yang, Yizhen Tian, Qingqing Zhang, Yongjie Wu, Shuhong Dong^{**}, Baolai Zhang^{*}

Department of Pharmacology, School of Basic Medical Sciences, Lanzhou University, Lanzhou, 730000, China



ARTICLE INFO

Keywords:

Ribavirin
Metabolomics
Metabolites
Metabolic pathway
Lung cancer

ABSTRACT

Ribavirin is a common antiviral drug, especially for patients with hepatitis C. Our recent studies demonstrated that ribavirin showed anti-tumor activity in colorectal cancer and hepatocellular carcinoma, but its effects on lung cancer remains unclear. This study aimed to evaluate the anti-tumor activity of ribavirin against lung cancer and elucidate the underlying mechanism. We established orthotopic mouse model of lung cancer (LLC and GLC-82) and employed an ultra-high-performance liquid chromatography quadrupole time-of-flight mass spectrometry (UPLC-Q-TOF/MS)-based metabolomics approach. We found that ribavirin significantly inhibited the proliferation and colony formation of lung cancer cells. Tumor sizes of orthotopic lung cancer in ribavirin-treated groups were also significantly lower than those in control groups. Metabolomics analysis revealed that ribavirin mainly affected 5 metabolic pathways in orthotopic lung tumor models, taurine and hypotaurine metabolism, nicotinate and nicotinamide metabolism, linoleic acid metabolism, arginine biosynthesis and arachidonic acid metabolism. Furthermore, we identified 5 upregulated metabolites including β -nicotinamide adenine dinucleotide (NAD⁺), nicotinamide (NAM), taurine, ornithine and citrulline, and 7 downregulated metabolites including 1-methylnicotinamide (MNAM), S-adenosyl-L-homocysteine (SAH), N1-Methyl-2-pyridone-5-carboxamide (2PY), homocysteine (Hcy), linoleic acid, arachidonic acid (AA) and argininosuccinic acid in ribavirin-treated groups. These results provide new insight into the anti-tumor mechanism of ribavirin for lung cancer.

1. Introduction

Worldwide, lung cancer is the second most common cancer and the leading cause of cancer death. In 2020, GLOBOCAN estimated 2.21 million new cases (11.4% of total cancer cases) and 1.80 million deaths (18.0% of total cancer deaths). Despite recent advances, most patients with lung cancer present with an advanced stage with lack of curative therapy at diagnosis, leading to a very poor prognosis with 5-year survival rates of 10–20% [1]. In the last few decades, substantial evidence indicates that metabolic disorders play a key role in the pathogenesis of lung cancer. In this aspect, the development of drugs that regulate metabolic disorders as well as sensitive biomarkers for early detection of this malignancy help improve the outcome and survival rate for patients with lung cancer [2–4].

Ribavirin has been widely known as an antiviral drug and it can inhibit a variety of RNA and DNA viruses through suppressing the inosine-5' monophosphate dehydrogenase (IMPDH) [5]. The combination of ribavirin and interferon is commonly used in the treatment of chronic hepatitis C virus (HCV) infection [6]. Interestingly, recent studies have shown that bioactive components from plants exert both antiviral and anti-tumor activities [7–12]. Considering the link between antiviral activity and anti-tumor activities, several studies have evaluated the anti-tumor effects of ribavirin on thyroid tumors, breast cancer, glioblastoma and liver cancer, and the mechanism may be related to downregulating the expression of eukaryotic translation initiation factor 4E (eIF4E), inhibiting IMPDH function and modulating MAPK/ERK and EZH2 pathways [13–15]. In addition, previous studies by our group demonstrated that ribavirin can inhibit the growth of soft tissue

* Corresponding author. Department of Pharmacology, School of Basic Medical Sciences, Lanzhou University, No. 199 Donggang West Road, Lanzhou, 730000, Gansu Province, China.

** Corresponding author. Department of Pharmacology, School of Basic Medical Sciences, Lanzhou University, No. 199 Donggang West Road, Lanzhou, 730000, Gansu Province, China.

E-mail addresses: dongshh@lzu.edu.cn (S. Dong), zhangbl@lzu.edu.cn (B. Zhang).

¹ These authors contributed equally to this work.

sarcomas, colorectal cancer and hepatocellular carcinoma by down-regulating the expression of some members of the protein arginine methyltransferase (PRMT) family, such as type I PRMT1, PRMT4 and/or type II PRMT5 proteins [16–18]. Nevertheless, the metabolic mechanism responsible for the therapeutic efficacy of ribavirin on lung cancer is not clear.

Metabolomics is an emerging method that explores the metabolic characteristics of endogenous small-molecule metabolites (molecular weight <1000) involved in physiological or pathological conditions. The advantage of being more dynamic than the genome and transcriptome enables the metabolome to obtain more information about the changes of intracellular metabolites, and the characteristics of tumor metabolism using metabolomics has potential application in cancer diagnosis and therapy [19–21].

Therefore, in this study we aimed to evaluate the anti-tumor activity of ribavirin against lung cancer and elucidate the underlying mechanism using metabolomics approach. We established orthotopic mouse model of lung cancer and employed an ultra-high-performance liquid chromatography quadrupole time-of-flight mass spectrometry (UPLC-Q-TOF/MS) to identify the changes of lung cancer-related endogenous metabolites after treatment with ribavirin.

2. Materials and methods

2.1. Drugs and reagents

Ribavirin was purchased from J&K Scientific Ltd (Beijing, China). Chromatographic-grade ammonium hydroxide, acetonitrile ammonium, acetate and methanol were supplied from Merck & Co., Inc. (Darmstadt, Germany).

2.2. Cell lines and cell culture

Four lung cancer cell lines including A549, SPC-A-1, GLC-82 and Lewis lung cancer (LLC) were purchased from American Type Culture Collection, and cultured in RPMI-1640 (HyClone, UT, USA) supplemented with 1% antibiotics (HyClone, UT, USA) and 10% fetal bovine serum (Gibco, NY, USA), at 37 °C in a humidified 5% CO₂ incubator.

2.3. Cell proliferation assay

The MTT assay was performed to assess cell viability. Briefly, LLC, GLC-82, SPC-A-1 and A549 cells were seeded in 96-well plates at 2000 cells per well. Next day, cells were treated with ribavirin at specified concentrations for 0–4 day. The absorbance value at 570 nm was measured using ELx800 Absorbance Microplate Reader (Bio-TEK Instruments Inc., VT, USA).

2.4. Clonogenic assay

Lung cancer cells were plated in 60 mm dishes at 400 cells per dish and maintained for 15 ± 2 days. The colonies were then fixed with methanol solution for 20 min at room temperature and stained with 0.5% crystal violet solution for 20 min.

2.5. Animals

Male athymic BALB/c nude mice (6–7 weeks old) and male C57BL/6 (5–6 weeks old) mice were obtained from Shanghai SLAC Laboratory Animal Co., Ltd. (Shanghai, China) and Laboratory Animal Center of Lanzhou University (Lanzhou, China), respectively. Mice were bred and maintained in a specific pathogen free-rated environment with food and water ad libitum under light-controlled conditions. The animal experimental protocol was approved by the Animal Protection and Experiment Ethics Committee of Lanzhou University.

Lung cancer cells (LLC and GLC-82) were implanted into C57BL/6 or

BALB/c nude mice following the protocols previously described [22,23]. Briefly, mice were anesthetized with sodium pentobarbital (45–60 mg/kg, i.p.) and a 1-cm-long incision was made in the skin on their left side. Cells (1×10^6 cells/50 μ L) were then inoculated into the left lateral thorax using a disposable sterile insulin syringe (U-40) with 30-gauge needle. Next day, C57BL/6 or BALB/c mice were divided randomly into control (Ctrl, normal saline) and ribavirin (Rib, 100 mg/kg, i.p., 6 times/week) groups. After the indicated periods, all mice were sacrificed, left lungs were separated, and tumor size was measured. Tumor volumes were calculated according to the formula: V (mm^3) = $A \times B^2 \times 0.52$, A and B was the tumor long diameter and short diameter, respectively. The tumor volume inhibition rate (IR) was calculated as follows: $\text{IR} (\%) = (1 - \text{tumor volume of treatment group} / \text{tumor volume of control group}) \times 100\%$. One fraction of lung tumor tissues was fixed in 4% paraformaldehyde and the other fractions were stored at -80 °C.

2.6. Tumor sample preparation

Orthotopic lung tumor (GLC-82) tissues (70 mg) from BALB/c nude mice were grinded and mixed with 1 mL prechilled mixtures (V acetonitrile: V methanol: V water = 2:2:1). After being sonicated for 1 h on ice, the extracts were placed at -20 °C for 1 h and centrifuged at 16,000 g for 20 min at 4 °C. Subsequently, the supernatants were transferred into 2 mL LC/MS glass vials. Tumor quality control (QC) samples were generated by mixing 10 μ L from each experimental sample.

2.7. UPLC-MS/MS analysis

Chromatographic analysis of tumor samples was performed using an ultra-high-performance liquid chromatography quadrupole time-of-flight mass spectrometry (UPLC-Q-TOF/MS) system (1290 Infinity LC, Agilent Technologies, Santa Clara, CA, USA) equipped with a ACQUITY UPLC BEH column (2.1 \times 100 mm, 1.7 μ m, Waters, Ireland). The mobile phase contained: A = 25 mM NH₄Ac and 25 mM NH₄OH in water and B = acetonitrile. The whole chromatographic gradient: 0–0.5 min (95% B); 0.5–6.5 min (95%–65% B); 6.5–8.5 min (65%–40% B); 8.5–9.5 min (40% B); 9.5–10.6 min (40%–95% B); 10.6–15.6 min (95% B). The Triple TOF 5600 MS/MS (AB SCIEX, Framingham, MA, USA) was applied for MS detection. The electrospray ionization (ESI) source parameters were set as following: the source temperature 600 °C; the nebulizer gas and auxiliary gas were 60 psi; the curtain gas was 30 psi; the m/z range was 25–1200 Da; the IonSpray Voltage Floating was ± 5500 V; the accumulation time for product ion was 0.03 s/spectra. MS/MS data were acquired in the information dependent acquisition mode and high sensitivity modes. The declustering potential was ± 60 V, the collisional energy was 30 V with ± 15 eV. QC samples were placed into the column for data normalization during acquisition.

2.8. Data analysis of non-targeted metabolomics

MS-DIAL software (Version 4.48) was used to process the raw data including retention time correction, feature detection and alignment. The acceptable standard of method reproducibility and instrument stability was the relative standard deviations (RSDs) < 30%. The metabolites were identified by matching MS/MS data and molecular weight according to in-house MS2 database. SIMCA-P software (Version 14.0, Umetrics, Umeå, Sweden) was used for multivariate data analyses, including unsupervised principal component analysis (PCA) and orthogonal partial least squares discriminant analysis (OPLS-DA). The P -value was obtained by one-way analysis of variance (ANOVA) for multiple groups analysis. All differential metabolites between two groups were identified by using $FC > 2$ or < 0.5 , P -value < 0.05 and Variable Importance in Projection (VIP) > 1 derived from OPLS-DA. R package was used to cluster analyses for the identified differential metabolites. Metabolic pathways were established by MetaboAnalyst 5.0 (<http://www.metaboanalyst.ca/>).

2.9. Statistical analysis

Statistics analyses were performed using Microsoft Excel 2016 and the data were expressed as means \pm standard deviation (SD). The difference between two groups was analyzed using Student's t-test and P -values < 0.05 indicated statistically significant.

3. Results

3.1. Ribavirin inhibited the proliferation and colony formation of lung cancer cells

Lung cancer cells were treated with ribavirin (0, 12.5, 25 and 50 μM) for 0–4 day. Results showed that ribavirin significantly inhibited the proliferation and colony formation of lung cancer cells in a concentration-dependent manner (Fig. 1A and B).

3.2. Ribavirin suppressed the growth of orthotopic lung tumors in mice

Two orthotopic models of lung cancer were then established to evaluate the anti-tumor efficacy of ribavirin *in vivo*. The results showed that ribavirin significantly inhibited the growth of LLC orthotopic allograft tumors (IR = 88.67%, $P < 0.001$, Fig. 2A–C) and GLC-82 orthotopic xenograft tumors (IR = 72.76%, $P < 0.01$, Fig. 2D–F).

3.3. Endogenous metabolites changed in mouse model of orthotopic lung cancer treated with ribavirin

Next, we performed UPLC-Q-TOF/MS to identify the endogenous metabolites in two groups of mice (Control and Ribavirin). The typical chromatograms in both negative and positive ion modes (Supplementary Figs. S1 and S2) showed the difference between two groups in the total ion current map of the GLC-82 orthotopic lung tumors. Principal component analysis (PCA) of these metabolites showed that the samples of the control and ribavirin-treated group were divided into different areas in the PCA score plots (Fig. 3A). Moreover, QC samples were tightly clustered and distributed, indicating that the analysis system of

this experiment was stable and reliable. To explore the difference in metabolites between two groups, we used the orthogonal partial least squares discriminant analysis (OPLS-DA) for discriminant or classification analysis. The results showed that the samples of control and ribavirin groups could be separated in the OPLS-DA model (Fig. 3B), and demonstrated excellent discriminant ability ($R^2X = 0.491$, $R^2Y = 1$, $Q^2 = 0.847$). In particular, we confirmed the robustness of the OPLS-DA model through cross-validation, and the model parameters ($R^2 = 0.997$ and $Q^2 = 0.007$) were all within the requirements (Fig. 3C). The volcano plot was built to screen potential differential metabolites (Fig. 3D). Blue dots and red dots represented down-regulated and up-regulated metabolites, respectively.

3.4. Differential metabolites identification and metabolic pathways analysis

A total of 132 differential metabolites were obtained from the orthotopic lung tumors based on $VIP > 1.0$, $FC > 2.0$ or < 0.5 , and $P < 0.05$. Among these, 58 metabolites were increased, while 74 metabolites were decreased in ribavirin-treated group (Supplementary Table S1). Next, unsupervised clustering was performed by a cluster analysis heatmap to analyze the distribution trends of the differential metabolites. As shown in Fig. 4, the ribavirin group was concentrated in one cluster and separated from the control group, suggesting that ribavirin improved the metabolism of tumors in mice.

The differential metabolites were then imported into MetaboAnalyst 5.0 for pathway analysis. The pathways of impact value > 0.3 were regarded as the pathway of significant disturbance. Ribavirin mainly affected 5 metabolic pathways: Linoleic acid metabolism; Nicotinate and nicotinamide metabolism; Taurine and hypotaurine metabolism; Arginine biosynthesis and Arachidonic acid metabolism (Fig. 5 and Supplementary Table S2). Among key metabolites altered, the upregulated 5 metabolites were β -nicotinamide adenine dinucleotide (NAD^+), nicotinamide (NAM), taurine, ornithine and citrulline (Figs. 6 and 7), while the downregulated 7 metabolites were 1-methylnicotinamide (MNAM), S-adenosyl-L-homocysteine (SAH), N1-Methyl-2-pyridone-5-carboxamide (2PY), homocysteine (Hcy), linoleic acid, arachidonic

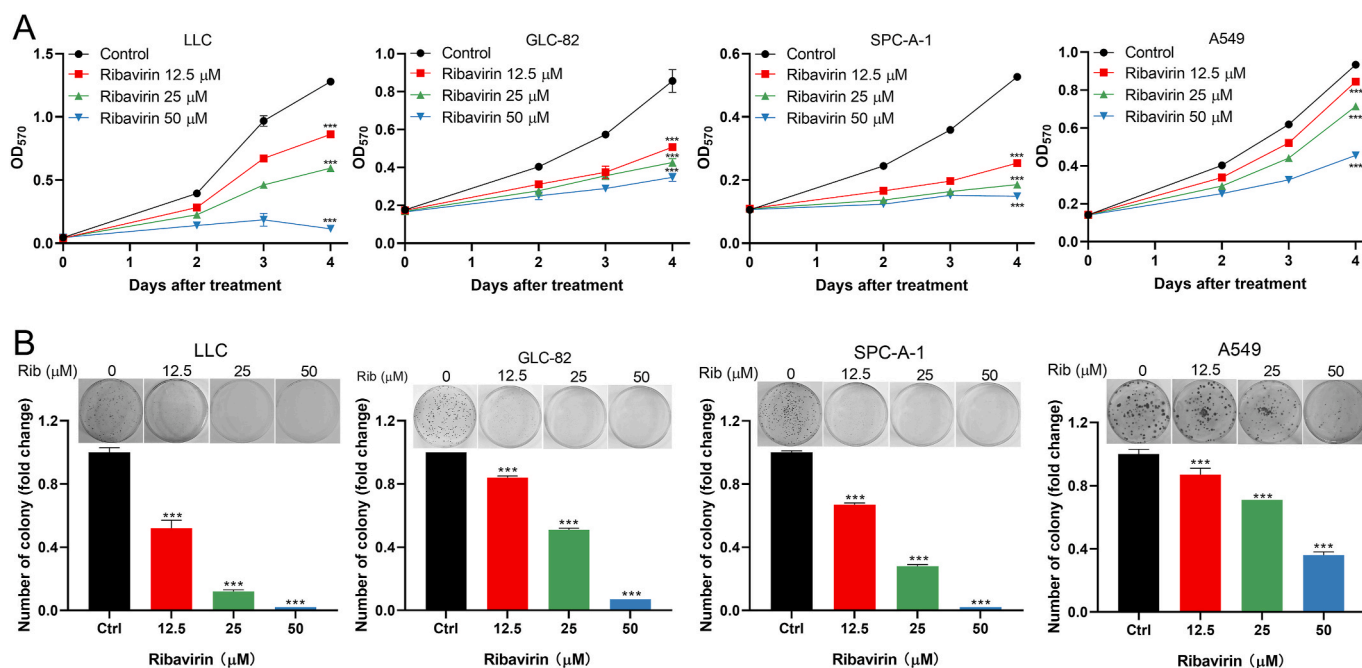


Fig. 1. Anti-tumor effects of ribavirin on lung cancer cells *in vitro*. (A) Lung cancer cells were treated with ribavirin as indicated, and cell proliferation was detected by MTT assay. (B) Lung cancer cells were treated with ribavirin as indicated for 15 ± 2 d, and colony formation was evaluated. Data were means \pm SD ($n = 3$). $***P < 0.001$.

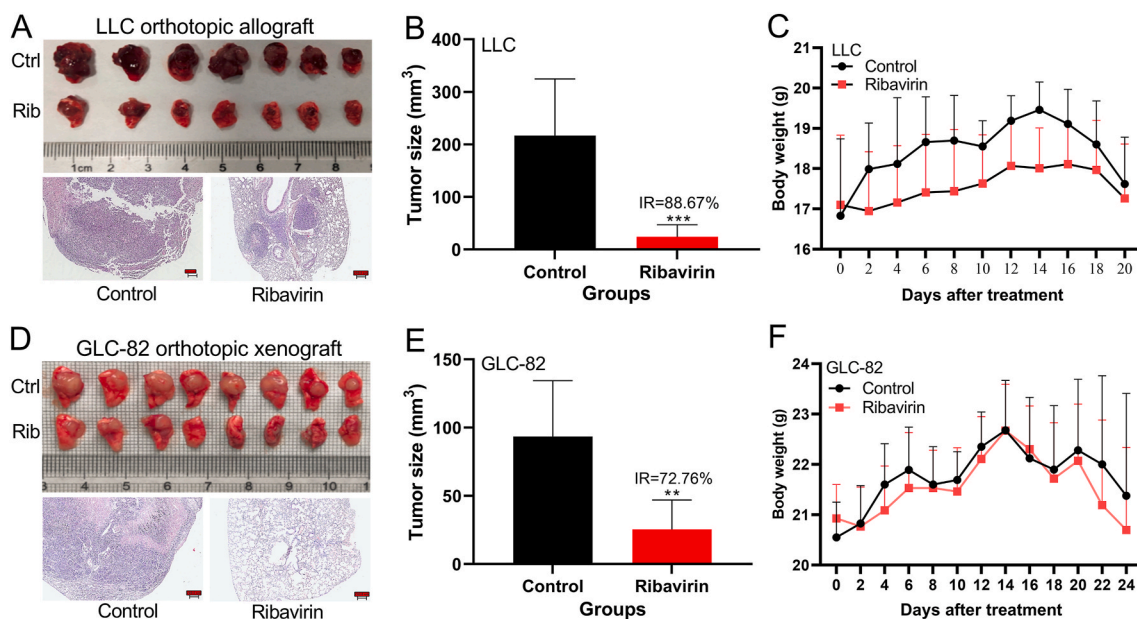


Fig. 2. Anti-tumor effects of ribavirin on orthotopic lung cancer models of mice. (A) Lungs derived from mice injected with LLC cells (magnification = 20 \times , scale bar = 200 μ m). (B) Mean size of tumors in mouse lungs inoculated with LLC cells. (C) The body weight of C57BL/6 mice. (D) Lungs derived from mice inoculated with GLC-82 cells (magnification = 20 \times , scale bar = 200 μ m). (E) Mean size of tumors in mouse lungs inoculated with GLC-82 cells. (F) The body weight of BALB/c nude mice.

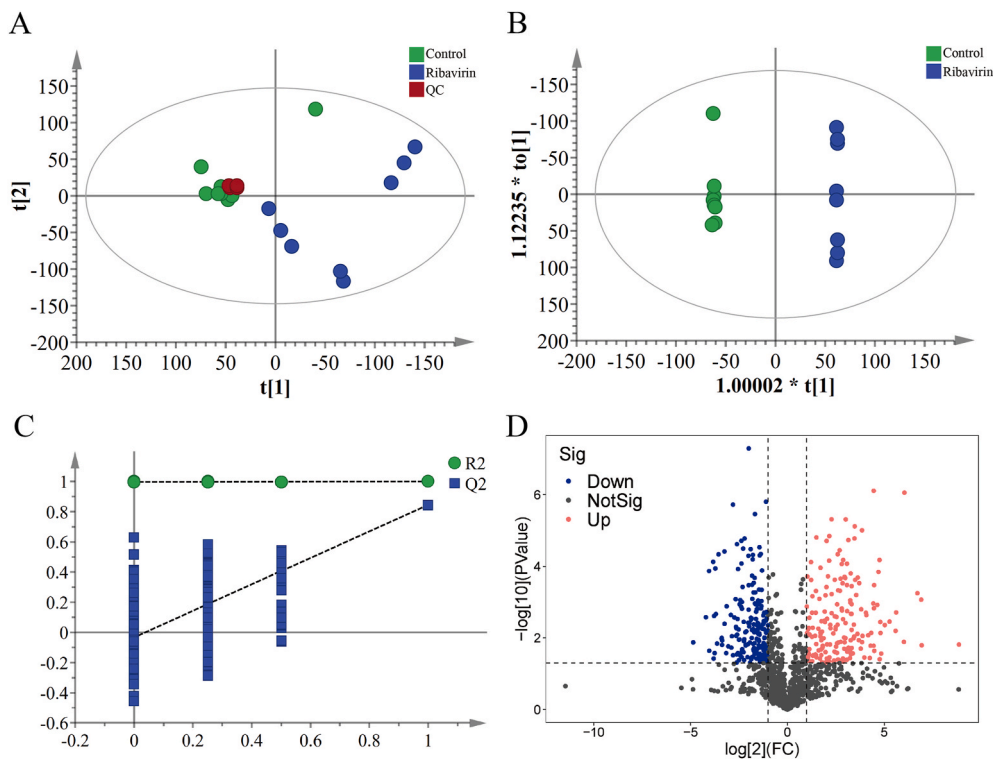


Fig. 3. Metabolomics analysis of orthotopic lung tumors in mice. (A) PCA score plots. (B) OPLS-DA score plots. (C) The permutation test plots from OPLS-DA. (D) The Volcano-Plot.

acid (AA) and argininosuccinic acid in ribavirin-treated group (Figs. 6 and 7).

4. Discussion

In this study, we showed that ribavirin significantly inhibited the cell viability and colony formation of lung cancer cells, and reduced the size

of GLC-82 and LLC orthotopic lung tumors. Moreover, we used a UPLC-Q-TOF/MS-based untargeted metabolomics approach to investigate the mechanisms by which ribavirin inhibited lung tumor. Ultimately, we identified 132 metabolites with significant alterations in orthotopic lung tumor after treatment with ribavirin, and revealed the changes in multiple metabolic pathways such as nicotinate and nicotinamide, taurine and hypotaurine and linoleic acid.

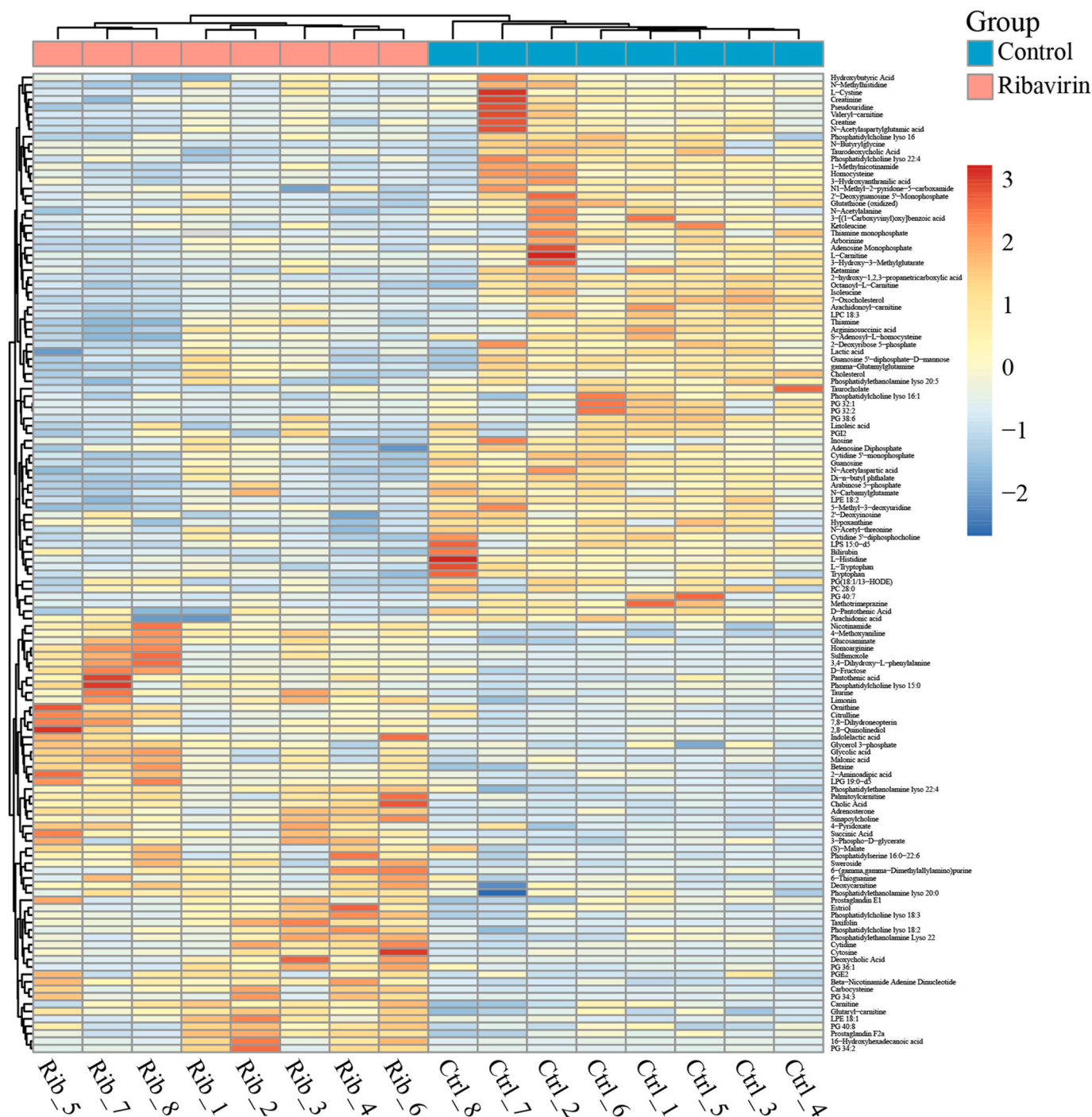


Fig. 4. Heatmap of the altered metabolites in orthotopic lung tumors after treatment with ribavirin. Red represents higher than average levels of differential metabolites and blue represents lower than average levels of differential metabolites. Columns represent tumor samples from mice and rows represent differential metabolites.

Nicotinamide (NAM) is a precursor of β -nicotinamide adenine dinucleotide (NAD^+) and can regulate cellular metabolism by participating in several redox and non-redox reactions [24,25]. Nicotinamide mononucleotide (NMN), which is an intermediate product from NAM to NAD^+ , acts as a co-enzyme in various redox reactions such as producing adenosine triphosphate or being phosphorylated to nicotinamide adenine dinucleotide phosphate ($NADP^+$). NAD^+ is also a substrate for enzymes involved in redox reactions in metabolic pathways, such as the poly ADP-ribose polymerase 1 (PARP1) and the sirtuin 1 (SIRT1) [24, 26]. In addition, nicotinamide N-methyltransferase (NNMT), a SAM-dependent cytoplasmic enzyme, catalyzes the N-methylation of

nicotinamide (NAM) taking SAM as a methyl donor to form SAH and N1-methylnicotinamide (MNAM). MNAM is then oxidized to the pyridones N1-methyl-2-pyridone-5-carboxamide (2PY) or N1-methyl-4-pyridone-3-carboxamide (4PY) by aldehyde oxidase (AOX) and excreted in urine, while S-adenosyl-L-homocysteine (SAH) is metabolized to the homocysteine (Hcy) [27–29].

Numerous studies have shown that NNMT is overexpressed in many types of cancer including lung cancer, colorectal cancer, gastric cancer and breast cancer, and is involved in tumor metastasis, leading to poor prognosis [28–31]. Moreover, NNMT can affect cell function by producing active metabolites and affecting the balance of cell methylation

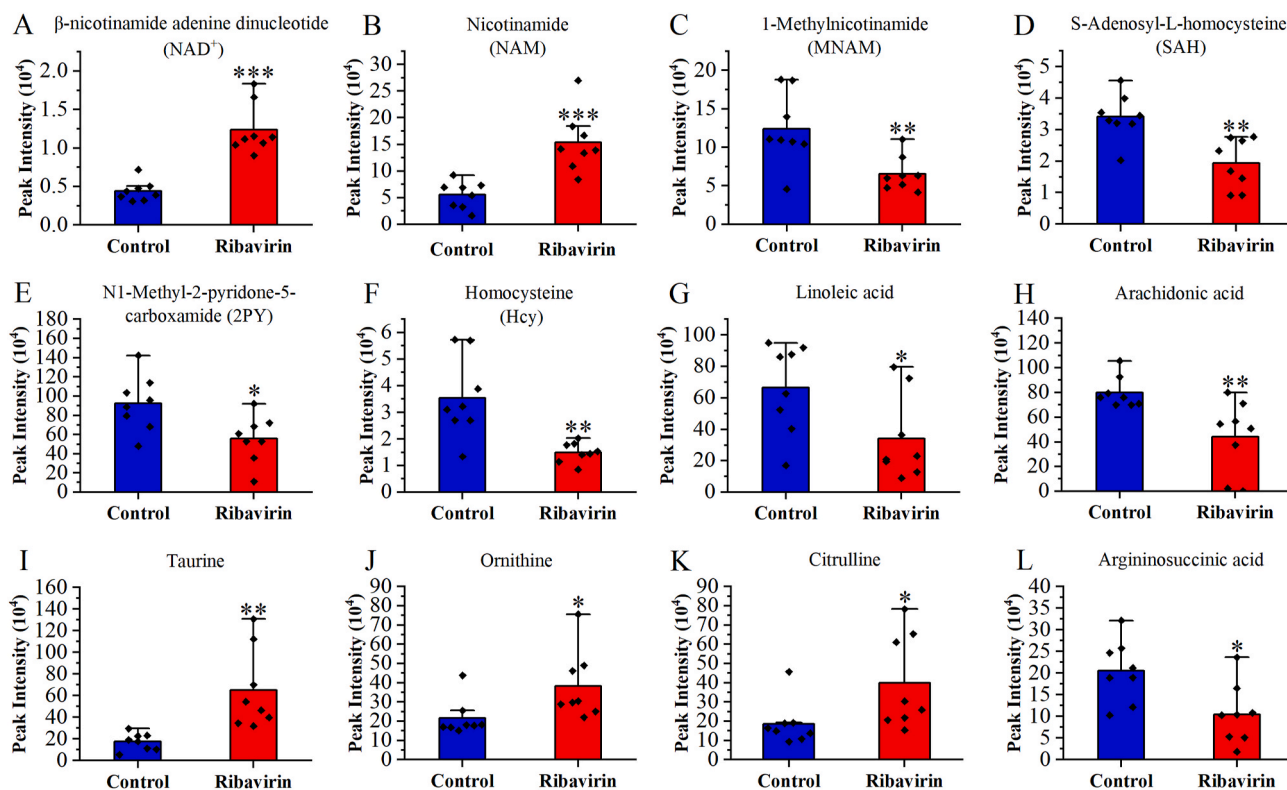


Fig. 7. The relative change of 12 key metabolites identified in orthotopic lung tumors after treatment with ribavirin. Data were means \pm SD. * $P < 0.05$. ** $P < 0.01$. *** $P < 0.001$.

metabolism of taurine and hypotaurine, nicotinate and nicotinamide, linoleic acid, arginine biosynthesis and arachidonic acid. Our findings provide new insight into the mechanism of ribavirin in lung cancer therapy.

Statement of ethics

Not applicable.

CRediT authorship contribution statement

Shihao Zhu: Validation, Software, Formal analysis, Writing–original draft. Xiang Han: Formal analysis, Writing – review & editing. Ruiying Yang: Methodology, Writing – review & editing. Yizhen Tian: Investigation, Data curation. Qingqing Zhang: Investigation. Yongjie Wu: Resources, Supervision. Shuhong Dong: Methodology, Investigation. Baolai Zhang: Conceptualization, Supervision, Writing – review & editing.

Declaration of competing interest

The authors declare that they have no known competing financial interests or personal relationships that could have appeared to influence the work reported in this paper.

Data availability

Data will be made available on request.

Acknowledgements

We thank Shanghai Bioprofile Technology Company Ltd. for UPLC-MS/MS analysis.

Appendix A. Supplementary data

Supplementary data to this article can be found online at <https://doi.org/10.1016/j.cbi.2022.110305>.

References

- [1] H. Sung, J. Ferlay, R.L. Siegel, M. Laversanne, I. Soerjomataram, A. Jemal, F. Bray, Global cancer statistics 2020: GLOBOCAN estimates of incidence and mortality worldwide for 36 cancers in 185 countries, *Ca - Cancer J. Clin.* 71 (2021) 209–249.
- [2] H. Gao, Y. Song, J. Ma, J. Zhai, Y. Zhang, X. Qu, Untargeted metabolomics analysis of omeprazole-enhanced chemosensitivity to cisplatin in mice with non-small cell lung cancer, *Chem. Biol. Interact.* 360 (2022), 109933.
- [3] Y. Bao, S. Wang, X. Yang, T. Li, Y. Xia, X. Meng, Metabolomic study of the intervention effects of Shuihonghuazi Formula, a Traditional Chinese Medicinal formulae, on hepatocellular carcinoma (HCC) rats using performance HPLC/ESI-TOF-MS, *J. Ethnopharmacol.* 198 (2017) 468–478.
- [4] H. Wu, L. Wang, X. Zhan, B. Wang, J. Wu, A. Zhou, A UPLC-Q-TOF/MS-based plasma metabolomics approach reveals the mechanism of Compound Kushen Injection-based intervention against non-small cell lung cancer in Lewis tumor-bearing mice, *Phytomedicine : Int. J. Phytother. Phytopharm.* 76 (2020), 153259.
- [5] P.M. Tate, V. Mastrodomenico, B.C. Mounce, Ribavirin induces polyamine depletion via nucleotide depletion to limit virus replication, *Cell Rep.* 28 (2019).
- [6] S. Slavenburg, Y.F. Heijdra, J.P.H. Drenth, Pneumonitis as a consequence of (peg) interferon-ribavirin combination therapy for hepatitis C: a review of the literature, *Dig. Dis. Sci.* 55 (2010) 579–585.
- [7] H.I. Mohamed, E.M. Fawzi, A. Basit, Kaleemullah, R. Lone, M.R. Sofy, Sorghum: nutritional factors, bioactive compounds, pharmaceutical and application in food systems: a review, *Phyton* 91 (2022) 1303–1325.
- [8] M. Butnariu, C. Quispe, J. Herrera-Bravo, J. Sharifi-Rad, L. Singh, N.M. Aborehab, A. Bouyahya, A. Venditti, S. Sen, K. Acharya, M. Bashiry, S.M. Ezzat, W.N. Setzer, M. Martorell, K.S. Mileski, I.C. Bagiu, A.O. Docea, D. Calina, W.C. Cho, The pharmacological activities of crocus sativus L.: a review based on the mechanisms and therapeutic opportunities of its phytoconstituents, 2022, *Oxid. Med. Cell. Longev.* (2022), 8214821.
- [9] M. Butnariu, C. Quispe, N. Koirala, S. Khadka, C.M. Salgado-Castillo, M. Akram, R. Anum, B. Yeskaliyeva, N. Cruz-Martins, M. Martorell, M. Kumar, R. Vasile Bagiu, A.F. Abdull Razis, U. Sunusi, R. Muhammad Kamal, J. Sharifi-Rad, Bioactive effects of curcumin in human immunodeficiency virus infection along with the most effective isolation techniques and type of nanoformulations, *Int. J. Nanomed.* 17 (2022) 3619–3632.

- [10] M. Butnariu, C. Cuique, J. Sharifi-Rad, E. Pons-Fuster, P. Lopez-Jornet, W. Zam, T. Das, A. Dey, M. Kumar, M. Pentea, H.E. A. A. Umbetova, J.T. Chen, Naturally-occurring bioactives in oral cancer: preclinical and clinical studies, bottlenecks and future directions, *Front. Biosci.* 14 (2022) 24.
- [11] M. Butnariu, C. Cuique, J. Herrera-Bravo, P. Helon, W. Kukula-Koch, V. López, F. Les, C.V. Vergara, P. Alarcón-Zapata, B. Alarcón-Zapata, M. Martorell, M. Pentea, A.A. Dragunescu, I. Samfira, Z. Yessimsiitova, S.D. Daştan, C.M. S. Castillo, T.H. Roberts, J. Sharifi-Rad, W. Koch, W.C. Cho, The effects of thymoquinone on pancreatic cancer: evidence from preclinical studies, *Biomed. Pharmacother. Biomed. pharmacotherapie* 153 (2022), 113364.
- [12] R. Yang, S. Dong, J. Zhang, S. Zhu, G. Miao, B. Zhang, Downregulation of PRMT5 by AMI-1 enhances therapeutic efficacy of compound kushen injection in lung carcinoma *in vitro* and *in vivo*, *Mol. Cell. Biochem.* (2022).
- [13] J. Casaos, N.L. Gorelick, S. Huq, J. Choi, Y. Xia, R. Serra, R. Felder, T. Lott, R. E. Kast, I. Suk, H. Brem, B. Tyler, N. Skuli, The use of ribavirin as an anticancer therapeutic: will it go viral? *Mol. Cancer Therapeut.* 18 (2019) 1185–1194.
- [14] F. Volpin, J. Casaos, J. Sesen, A. Mangraviti, J. Choi, N. Gorelick, J. Frikeche, T. Lott, R. Felder, S.J. Scotland, T.S.K. Eisinger-Mathason, H. Brem, B. Tyler, N. Skuli, Use of an anti-viral drug, Ribavirin, as an anti-glioblastoma therapeutic, *Oncogene* 36 (2017) 3037–3047.
- [15] F. Pettersson, S.V. Del Rincon, A. Emond, B. Huor, E. Ngan, J. Ng, M.C. Dobocan, P. M. Siegel, W.H. Miller, Genetic and pharmacologic inhibition of eIF4E reduces breast cancer cell migration, invasion, and metastasis, *Cancer Res.* 75 (2015) 1102–1112.
- [16] S. Ge, Q. Zhang, Y. Chen, Y. Tian, R. Yang, X. Chen, F. Li, B. Zhang, Ribavirin inhibits colorectal cancer growth by downregulating PRMT5 expression and H3R8me2s and H4R3me2s accumulation, *Toxicol. Appl. Pharmacol.* 415 (2021), 115450.
- [17] Y. Tian, W. Yang, R. Yang, Q. Zhang, L. Hao, E. Bian, Y. Yang, X. Huang, Y. Wu, B. Zhang, Ribavirin inhibits the growth and ascites formation of hepatocellular carcinoma through downregulation of type I CARM1 and type II PRMT5, *Toxicol. Appl. Pharmacol.* 435 (2022), 115829.
- [18] Q. Zhang, R. Yang, Y. Tian, S. Ge, X. Nan, S. Zhu, S. Dong, B. Zhang, Ribavirin inhibits cell proliferation and metastasis and prolongs survival in soft tissue sarcomas by downregulating both protein arginine methyltransferases 1 and 5, *Basic Clin. Pharmacol. Toxicol.* 131 (2022) 18–33.
- [19] A.K. Kaushik, R.J. DeBerardinis, Applications of metabolomics to study cancer metabolism, *Biochim. Biophys. Acta Rev. Canc* (2018) 1870.
- [20] E. Arslan, I. Koyuncu, Comparison of amino acid metabolisms in normal prostate (PNT-1A) and cancer cells (PC-3), *Oncologie* 23 (2021) 105–117.
- [21] D. Zhang, L. Tong, Q. Wang, Y. Cao, Y. Gao, D. Yang, T. Bao, Z. Zhu, Diagnosis of lung cancer based on plasma metabolomics combined with serum markers, *Oncologie* 22 (2020) 75–82.
- [22] Z. Gu, S. Gao, F. Zhang, Z. Wang, W. Ma, R.E. Davis, Z. Wang, Protein arginine methyltransferase 5 is essential for growth of lung cancer cells, *Biochem. J.* 446 (2012) 235–241.
- [23] S. Sakamoto, H. Inoue, S. Ohba, Y. Kohda, I. Usami, T. Masuda, M. Kawada, A. Nomoto, New metastatic model of human small-cell lung cancer by orthotopic transplantation in mice, *Cancer Sci.* 106 (2015) 367–374.
- [24] I.P. Nikas, S.A. Paschou, H.S. Ryu, The role of nicotinamide in cancer chemoprevention and therapy, *Biomolecules* 10 (2020).
- [25] E.S. Hwang, S.B. Song, Nicotinamide is an inhibitor of SIRT1 *in vitro*, but can be a stimulator in cells, *Cell. Mol. Life Sci. : CM* 74 (2017) 3347–3362.
- [26] W. Wang, C. Yang, T. Wang, H. Deng, Complex roles of nicotinamide N-methyltransferase in cancer progression, *Cell Death Dis.* 13 (2022) 267.
- [27] P. Pissios, Nicotinamide N-methyltransferase: more than a vitamin B3 clearance enzyme, *Trends Endocrinol. Metabol. : TEM (Trends Endocrinol. Metab.)* 28 (2017) 340–353.
- [28] D. Sartini, S. Morganti, E. Guidi, C. Rubini, A. Zizzi, R. Giuliante, V. Pozzi, M. Emanuelli, Nicotinamide N-methyltransferase in non-small cell lung cancer: promising results for targeted anti-cancer therapy, *Cell Biochem. Biophys.* 67 (2013) 865–873.
- [29] R.B. Parsons, P.D. Facey, Nicotinamide N-methyltransferase: an emerging protagonist in cancer macro(r)evolution, *Biomolecules* 11 (2021).
- [30] A. Roberti, A.F. Fernández, M.F. Fraga, Nicotinamide N-methyltransferase: at the crossroads between cellular metabolism and epigenetic regulation, *Mol. Metabol.* 45 (2021), 101165.
- [31] S. Tatekawa, K. Ofusa, R. Chijimatsu, A. Vecchione, K. Tamari, K. Ogawa, H. Ishii, Methyltransferase system for cancer sieging strategy, *Cancers* 13 (2021).
- [32] O.A. Ulanovskaya, A.M. Zuhl, B.F. Cravatt, NNMT promotes epigenetic remodeling in cancer by creating a metabolic methylation sink, *Nat. Chem. Biol.* 9 (2013) 300–306.
- [33] B. Choque, D. Catheline, V. Rioux, P. Legrand, Linoleic acid: between doubts and certainties, *Biochimie* 96 (2014) 14–21.
- [34] J.S. Hamilton, E.L. Klett, Linoleic acid and the regulation of glucose homeostasis: a review of the evidence, *Prostaglandins Leukot. Essent. Fatty Acids* 175 (2021), 102366.
- [35] C. Ruiying, L. Zeyun, Y. Yongliang, Z. Zijia, Z. Ji, T. Xin, Z. Xiaojian, A comprehensive analysis of metabolomics and transcriptomics in non-small cell lung cancer, *PLoS One* 15 (2020), e0232272.
- [36] Y. Chen, Z. Ma, A. Li, H. Li, B. Wang, J. Zhong, L. Min, L. Dai, Metabolomic profiling of human serum in lung cancer patients using liquid chromatography/hybrid quadrupole time-of-flight mass spectrometry and gas chromatography/mass spectrometry, *J. Cancer Res. Clin. Oncol.* 141 (2015) 705–718.
- [37] J. de Castro, M.C. Rodríguez, V.S. Martínez-Zorzano, M. Llanillo, J. Sánchez-Yagüe, Platelet linoleic acid is a potential biomarker of advanced non-small cell lung cancer, *Exp. Mol. Pathol.* 87 (2009) 226–233.
- [38] J.X. Wang, Y. Li, L.K. Zhang, J. Zhao, Y.Z. Pang, C.S. Tang, J. Zhang, Taurine inhibits ischemia/reperfusion-induced compartment syndrome in rabbits, *Acta Pharmacol. Sin.* 26 (2005) 821–827.
- [39] S. Baliou, A.M. Kyriakopoulos, D.A. Spandidos, V. Zoumpourlis, Role of taurine, its haloamines and its lncRNA TUG1 in both inflammation and cancer progression. On the road to therapeutics? (Review), *Int. J. Oncol.* 57 (2020) 631–664.
- [40] J.M. Hu, H.T. Sun, Serum proton NMR metabolomics analysis of human lung cancer following microwave ablation, *Radiat. Oncol.* 13 (2018) 40.
- [41] S. Xu, Y. Zhou, H. Geng, D. Song, J. Tang, X. Zhu, D. Yu, S. Hu, Y. Cui, Serum metabolic profile alteration reveals response to platinum-based combination chemotherapy for lung cancer: sensitive patients distinguished from insensitive ones, *Sci. Rep.* 7 (2017), 17524.
- [42] W. Wang, J. Lv, N. Chen, B. Lou, W. Mao, P. Wang, Y. Chen, Dysregulated serum metabolites in staging of hepatocellular carcinoma, *Clin. Biochem.* 61 (2018) 7–11.
- [43] I.M. El Agouza, S.S. Eissa, M.M. El Houseini, D.E. El-Nashar, O.M. Abd El Hameed, Taurine: a novel tumor marker for enhanced detection of breast cancer among female patients, *Angiogenesis* 14 (2011) 321–330.
- [44] F. Wang, N. Ma, F. He, S. Kawanishi, H. Kobayashi, S. Oikawa, M. Murata, Taurine attenuates carcinogenicity in ulcerative colitis-colorectal cancer mouse model, 2020, *Oxid. Med. Cell. Longev.* (2020), 7935917.
- [45] X. Zhang, C. Bi, Y. Fan, Q. Cui, D. Chen, Y. Xiao, Q.P. Dou, Induction of tumor cell apoptosis by taurine Schiff base copper complex is associated with the inhibition of proteasomal activity, *Int. J. Mol. Med.* 22 (2008) 677–682.
- [46] Y.U. He, Q.Q. Li, S.C. Guo, Taurine attenuates dimethylbenz[a]anthracene-induced breast tumorigenesis in rats: a plasma metabolomic study, *Anticancer Res.* 36 (2016) 533–543.
- [47] Y. Deng, H. Li, Y. Tang, The effect of suppression taurine on relocation and epithelial-mesenchymal transition in mankind lung cancer cells, 2021, *J. Health. Eng.* (2021), 6656080.
- [48] M.J. Lukey, W.P. Katt, R.A. Cerione, Targeting amino acid metabolism for cancer therapy, *Drug Discov. Today* 22 (2017) 796–804.
- [49] F. Qiu, J. Huang, M. Sui, Targeting arginine metabolism pathway to treat arginine-dependent cancers, *Cancer Lett.* 364 (2015) 1–7.
- [50] S. Rabinovich, L. Adler, K. Yizhak, A. Sarver, A. Silberman, S. Agron, N. Stettner, Q. Sun, A. Brandis, D. Helbling, S. Korman, S. Itzkovitz, D. Dimmock, I. Ulitsky, S. C. Nagamani, E. Ruppin, A. Erez, Diversion of aspartate in ASS1-deficient tumours fosters de novo pyrimidine synthesis, *Nature* 527 (2015) 379–383.